Supplemental data

dNPF-GAL4 does not label cell bodies in the ventral ganglion.

We demonstrated that stimulating *dNPF*-expressing neurons for 30 min prior to testing mimicked the effects of food-deprivation. The *dNPF*-GAL4 driver used in these experiments labels the dNPF-immunoreactive neurons in the dorsal brain but not those in the subesophageal ganglion. We also imaged the ventral ganglion of flies expressing uas-*CD8::GFP* driven by *dNPF*-GAL4. This analysis revealed that *dNPF*-GAL4 labels projections from two neurons in brain that decend into the ventral ganglion but it does not label any cell bodies within the ventral ganglion. Therefore our experiments are controlling the activity of the neurons whose cell bodies reside in the dorsal and lateral protocerebrum.

Experimental Procedures

Fly strains

Fly stocks were raised on standard cornmeal food at 23°C and 60% relative humidity. The wild-type *Drosophila* strain used in this study was Canton-S. The *dNPF* (Wen et al., 2005), c061 (www.flytrap.org), 210Y, c005, 104Y (Liu et al., 2006) , OK107 (Connolly et al., 1996) MB247 (Zars et al., 2000), *TH*-GAL4 (Friggi-Grelin et al., 2003), NP2758 (Tanaka et al., 2008) and *krasavietz* (Dubnau et al., 2003; Shang et al., 2007) GAL4 lines are described. *n*-synaptobrevin-GAL4 flies were a gift from Julie Simpson (HHMI Janelia Farm Research

Campus). c061 and *krasavietz* were combined with the previously described MBGAL80 transgene (Krashes et al., 2007). The uas-*npfr1*^{RNAi} (Wu et al., 2003), uas-*dcr2* (Dietzl et al., 2007), *TH*GAL80 (Sitaraman et al., 2008), uas-*shi*^{ts1} (Kitamoto, 2001), uas-*dTrpA1* (Hamada et al., 2008) and MB-DsRED (Riemensperger et al., 2005) flies are described. *TH*GAL80 was combined with uas-*shi*^{ts1} on the 3rd chromosome.

Table S1. Sensory Acuity of strains used in this study. All genotypes were either tested for odor acuity at 23˚C or at the restrictive temperature for uas-*shi*^{ts1} or uas-*dTrpA1* of 31°C. All genotypes were tested for sucrose acuity at the permissive temperature of 23°C. No statistical differences were apparent between the relevant groups. (OCT 23˚C P>0.98; MCH 23˚C P>0.80; OCT 31˚C P>0.88; MCH 31˚C P>0.99; sucrose P>0.89). All n≥6.

Supplemental Figure Legends

Figure S1. *dNPF*-GAL4 does not label somata in the ventral ganglion. *dNPF*-GAL4 driven CD8::GFP (green) shows strong expression in the brain and fibres descending into the ventral ganglion. However, no somata are labeled in the ventral ganglion. Scale bar represents 50μm.

Figure S2. Silencing *npfr1* in all neurons specifically disrupts 3 hr appetitive olfactory memory. A. Driving the uas-*npfr1*^{RNAi} globally throughout the brain using syb-GAL4 in the presence or absence of uas-*dicer2* attenuates memory performance in hungry animals. uas-*npfr1*^{RNAi}/syb-GAL4 and uas-*dcr2*;

npfr1^{RNAi}/syb-GAL4 flies are statistically different than wild-type, uas-*npfr1*^{RNAi}, syb-GAL4, uas-*dcr2*, uas-*dcr2*; syb-GAL4/+ and uas-*dcr2*; uas-*npfr1*^{RNAi} controls. **B.** Driving the uas-*npfr1*^{RNAi} globally throughout the brain using syb-GAL4 in the presence or absence of uas-*dicer2* does not affect 3 minute aversive memory performance. Data are mean ± SEM. Asterisks denote significant difference ($P<0.05$, ANOVA) from other unmarked groups. Data are mean ± SEM.

Figure S3. MB-MP neurons do not contain GABA or acetylcholine. A. The separate and merged channels from confocal images of a PPL1 cluster in a c061;MBGAL80;uas-*CD8::GFP* brain counter-labeled with GFP (green) and an anti-GABA antibody (red). **B.** The separate and merged channels of a confocal image at the level of the MB heel in an NP2758;uas-*CD8::GFP* brain counter-labeled with GFP (green) and anti-TH antibody (red) and anti-ChAT (choline acetyl transferase) antibody. GFP strongly labels the heel region of the MB (white arrow). This region is also innervated by dopaminergic processes in the anti-TH labeled image. Anti-TH also strongly labels dopaminergic neuron cell bodies at that level of the brain (white arrow head). Anti-ChAT strongly labels many processes in the brain but is notably absent from the heel region of the MB. Scale bar represents 10μm.

Figure S4. Analysis of expression in subsets of dopaminergic neurons.

A. A projection view of frontal sections from a brain containing labeled dopaminergic neurons with *TH*-GAL4 driven uas-*CD8::GFP* reveals dense

innervation of specific domains in the dorsal protocerebrum including the heel of the MB (yellow arrows). **B.** Quantification of the number of anti-TH labeled neurons and GFP-positive neurons in the PPL1 cluster of the three GAL4 lines, c061;MBGAL80, MBGAL80;*krasavietz* and NP2758, used in this study. Data are mean ± SEM. n=16 PPL1 clusters from 8 brains per genotype. **C.** The MBGAL80;*krasavietz* line labels two MB-MP neurons and one additional dopaminergic neuron in each PPL1 cluster that projects to the stalk of the α lobe. Projection view of a MBGAL80;*krasavietz*/uas-*CD8::GFP* brain reveals the MB-MP neuron processes in the heel of the MB (yellow arrows) as well as projections from other neurons on the stalk of the MB α lobe (blue arrows). **D.** Projection view of a MBGAL80/*TH*GAL80;*krasavietz*/uas-*CD8::GFP* brain reveals that the *TH*GAL80 transgene removes expression from the MB-MP neurons and the neurons projecting to the stalk of the α lobe (hollow arrows). Scale bar represents 20μm.

Figure S5. Blocking only 2 or 4 of the 6 MB-MP neurons does not release appetitive memory performance in fed flies. A. Feeding flies after training suppresses 3 hr memory performance of all groups used in this experiment. All genotypes were food-deprived, trained, fed and tested at the permissive temperature of 23˚C. **B.** Blocking synaptic output from 6 MB-MP neurons with c061; MBGAL80 for one hour before testing using uas-*shi*^{ts1} reveals memory performance in satiated flies but blocking 4 with MBGAL80;*krasavietz* or 2 with NP2758 does not. Memory performance of MBGAL80;*krasavietz*/uas-*shi*^{ts1}

(PI=0.09±0.03) and NP2758; uas-*shi*^{ts1} flies (PI=0.03±0.07) was statistically indistinguishable from all groups (all P>0.24) except c061;MBGAL80; uas-*shi*^{ts1} flies (both P<0.04). All genotypes were food-deprived, trained and stored in food vials for 120min at 23˚C. Vials were then shifted to 31˚C for 60min before flies were tested for appetitive memory at 31˚C. Data are mean ± SEM.

Figure S6. Stimulating MB-MP neurons during testing suppresses appetitive memory performance but stimulating during acquisition or temporarily after training does not. A. All genotypes were food-deprived, trained and stored in food vials for 120min at 23˚C. Vials were then shifted to 31˚C for 15min before flies were tested for appetitive memory at 31˚C. **B.** All genotypes were food-deprived and trained at 23˚C. They were then immediately transferred to food vials at 31˚C for 60min and returned to 23˚C for 120min before being tested for memory at 23˚C. **C.** All genotypes were food-deprived at 23˚C and 30min before training they were transferred to 31˚C and trained. After training they were stored in food vials for 180min at 23˚C before flies were tested for appetitive memory at 23˚C. Asterisk denotes significant difference (P<0.05, ANOVA) from other unmarked groups. Data are mean ± SEM.

Figure S7. Blocking all DA neurons impairs acquisition of aversive odor memory but blocking MB-MP neurons does not. All flies were incubated at 31˚C for 30min before and during training with the aversive odor and shock protocol. Immediately after training all flies were returned to 23˚C and tested for 3

hr aversive odor memory. Asterisk denotes significant difference (P<0.002, ANOVA) from other unmarked groups. Data are mean ± SEM.

Supplemental Movies

Movie S1. A 3-dimensional projection view of a confocal stack of a c061;MBGAL80/uas-*CD8::GFP*;MB-DsRed brain. To produce this movie the green channel was thresholded to reveal the projections of MB-MP neurons in more detail. Thresholding made the neurons that project to the fan-shaped body of the central complex invisible.

Movie S2. A 3D volume rendered view of a c061;MBGAL80/uas-*CD8::GFP*;MB-DsRed brain using Amira software.

Movie S3. A 3-dimensional projection view of a confocal stack of an NP2758;uas-*CD8::GFP*;MB-DsRed brain.

Movie S4. A 3D volume rendered view of an NP2758;uas-*CD8::GFP*;MB-DsRed brain using Amira software.

Movie S5. A 3-dimensional projection view of confocal stack of an MBGAL80/ uas-*CD8::GFP;* krasavietz/MB-DsRed brain.

Movie S6. A 3D volume rendered view of an MBGAL80/uas-*CD8::GFP;* krasavietz/MB-DsRed brain using Amira software.

Table S1

	OCT		MCH		sucrose acuity
	23ÞC	31ÞC	23ÞC	31ÞC	23ÞC
uas-npfr1RNAi	0.51+/-0.06		0.60+/-0.07		0.61+/-0.05
c061	0.52+/-0.03		0.59+/-0.10		0.57+/-0.08
c061; uas-npfr1RNAi	0.57+/-0.05		0.55+/-0.09		0.59+/-0.08
syb-GAL4	0.56+/-0.06		0.57+/-0.05		0.61+/-0.05
uas-dcr2; syb-GAL4	0.54+/-0.06		0.53+/-0.07		-
uas-dcr2	0.51+/-0.04		0.53+/-0.06		-
uas-dcr2;uas-npfr1RNAi	0.56+/-0.08		0.55+/-0.05		0.58+/-0.04
uas-dcr2;uas-npfr1RNAi;syb-GAL4	0.52+/-0.06		0.63+/-0.08		0.65+/-0.06
uas-npfr1RNAi/TH-GAL4	0.61+/-0.09		0.70+/-0.07		0.60+/-0.07
wild-type		0.52+/-0.03		0.59+/-0.11	0.59+/-0.04
uas-shi		0.51+/-0.03		0.63+/-0.10	0.62+/-0.05
c061; MBGAL80		0.54+/-0.05		0.60+/-0.11	0.62+/-0.05
c061; MBGAL80; uas-shi		0.57+/-0.11		0.64+/-0.10	0.62+/-0.06
NP2758		0.62+/-0.09		0.53+/-0.06	0.61+/-0.05
NP2758; uas-shi		0.55+/-0.05		0.58+/-0.04	0.65+/-0.02
MBGAL80; krasavietz		0.65+/-0.07		0.57+/-0.03	0.59+/-0.07
MBGAL80; krasavietz/ uas-shi		0.56+/-0.03		0.56+/-0.03	0.64+/-0.10
THGAL80; uas-shi		0.56+/-0.06		0.59+/-0.06	0.64+/-0.07
c061; MBGAL80/THGAL80; uas-shi		0.54+/-0.02		0.56+/-0.04	0.67+/-0.06
uas-dTRPA1		0.51+/-0.06		0.65+/-0.10	0.58+/-0.09
dNPF-GAL4		0.50+/-0.04		0.60+/-0.07	0.69+/-0.05
c061; MBGAL80/uas-dTRPA1		0.56+/-0.07		0.60+/-0.12	0.59+/-0.07
dNPF-GAL4/uas-dTRPA1		0.51+/-0.05		0.57+/-0.09	0.70+/-0.03
NP2758; uas-dTRPA1		0.61+/-0.07		0.57+/-0.07	0.68+/-0.06
MBGAL80/uas-dTRPA1; krasavietz		0.64+/-0.08		0.54+/-0.03	0.61+/-0.04

Fig. S1

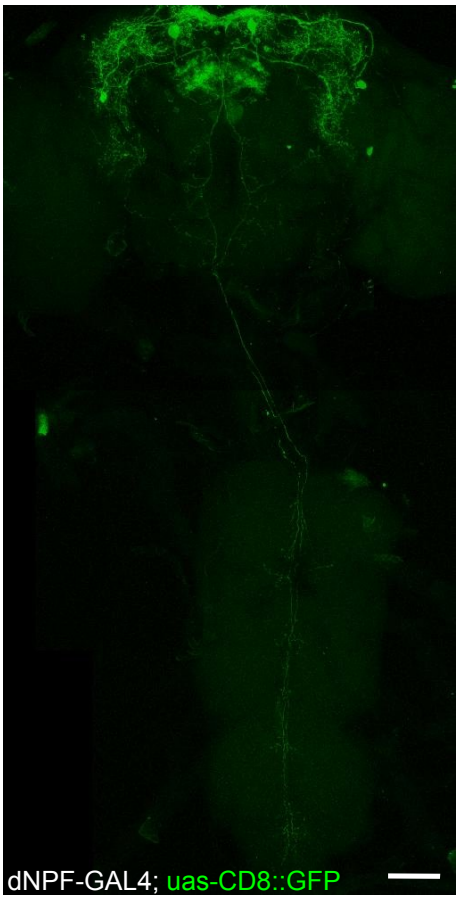

Fig. S2

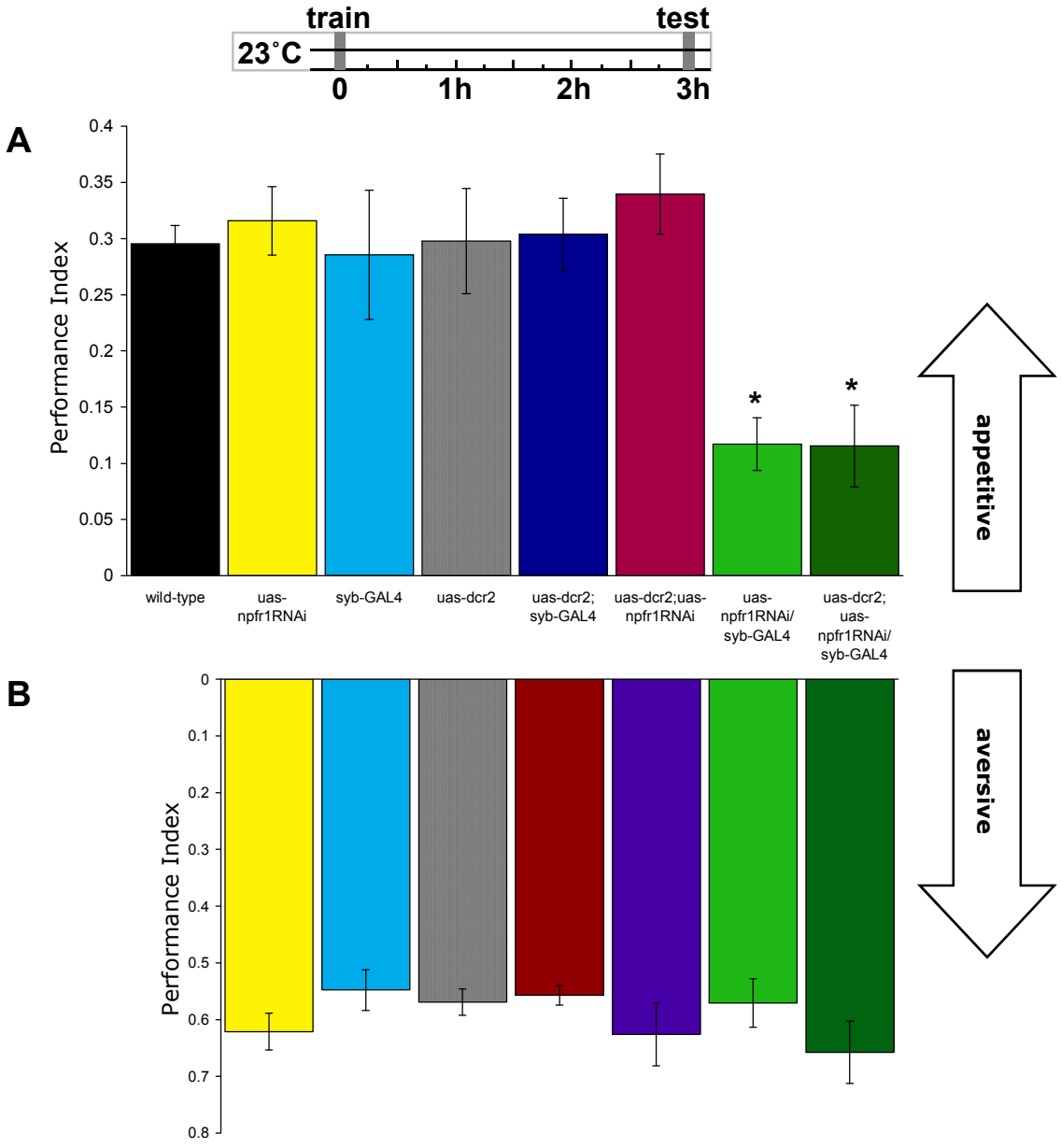
train
test
23˚C
0
1h
2h
3h
A
Performance Index
0.4
0.35
0.3
0.25
0.2
0.15
0.1
0.05
0
*
*
wild-type
uas-npfr1RNAi
syb-GAL4
uas-dcr2
uas-dcr2; syb-GAL4
uas-dcr2;uas-npfr1RNAi
uas-npfr1RNAi/ syb-GAL4
uas-dcr2; uas-npfr1RNAi/ syb-GAL4
appetitive
B
Performance Index
0
0.1
0.2
0.3
0.4
0.5
0.6
0.7
0.8
aversive

Fig. S3

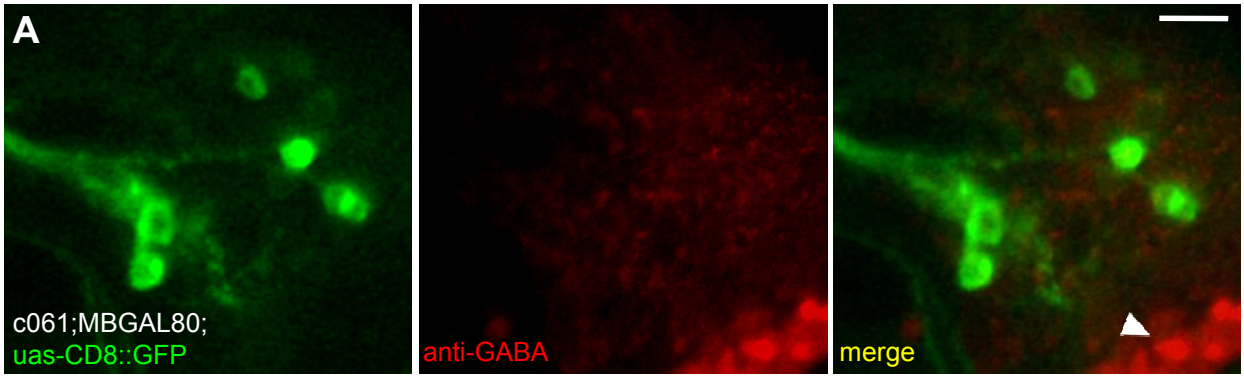
A
c061;MBGAL80;
uas-CD8::GFP
anti-GABA
merge

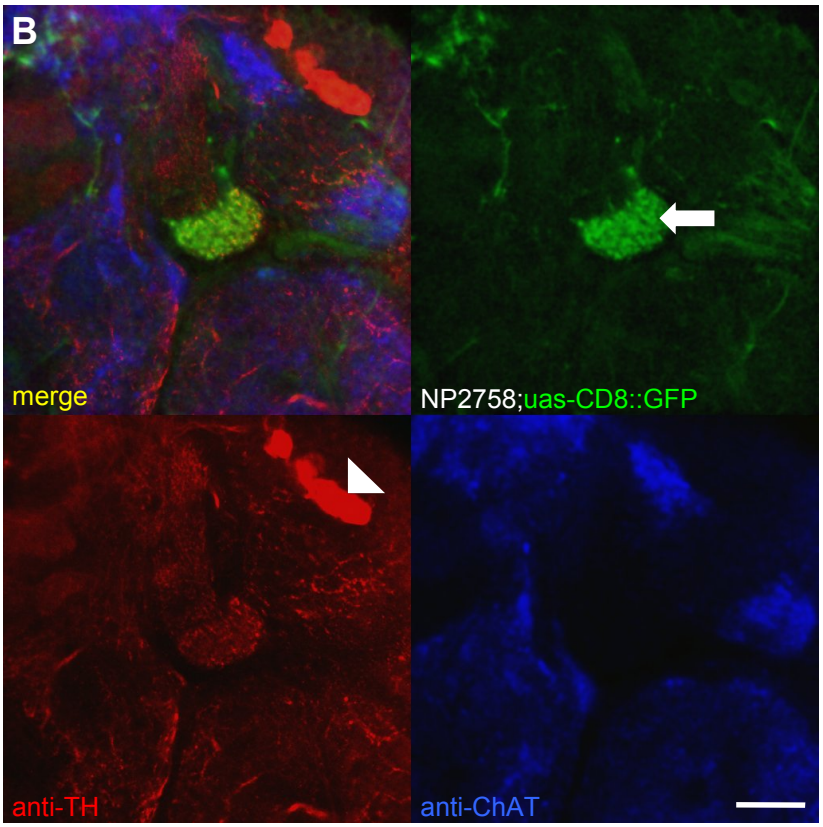
B
merge
NP2758;uas-CD8::GFP
anti-TH
anti-ChAT

Fig. S4

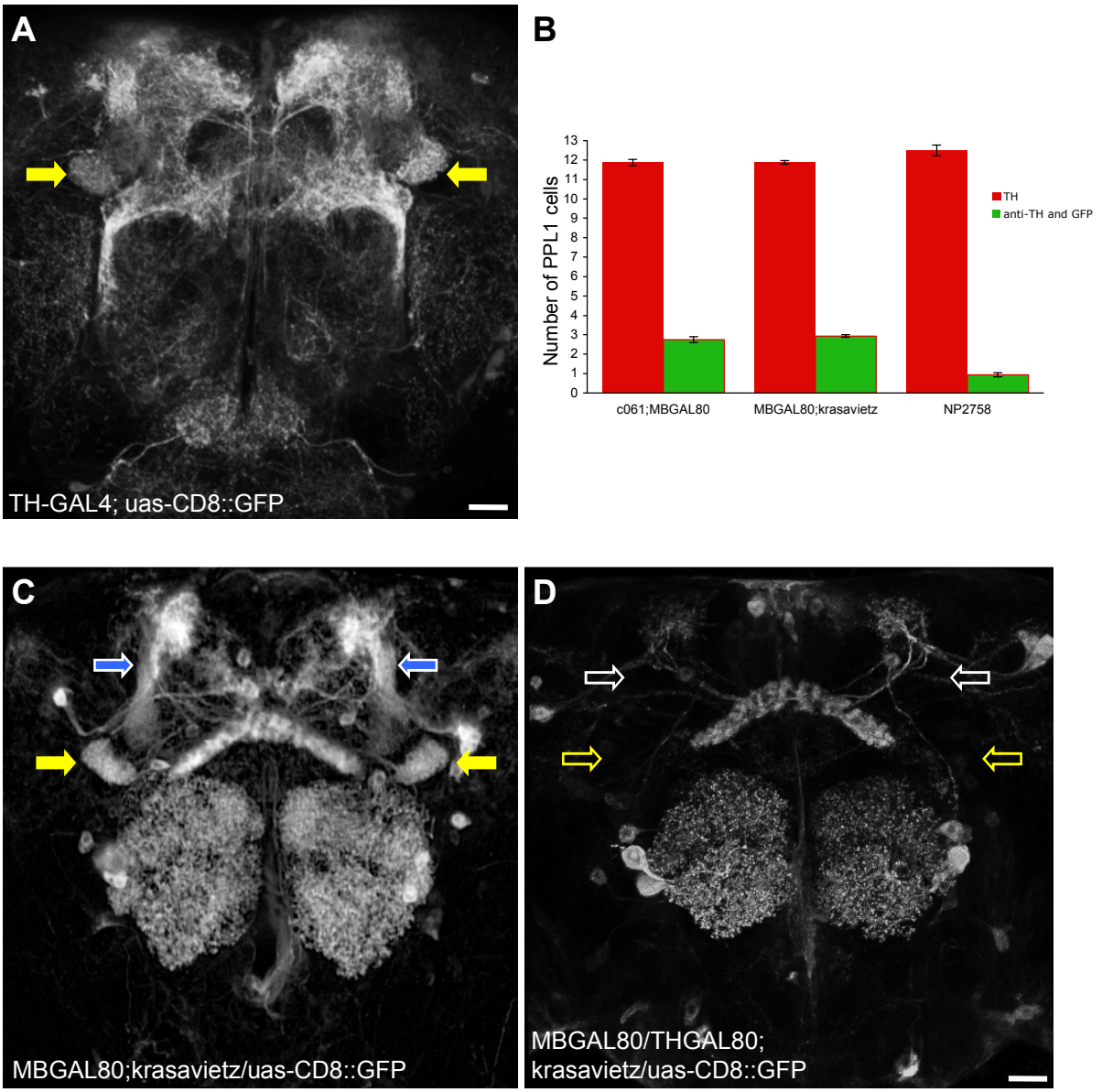
A
TH-GAL4; uas-CD8::GFP
B
Number of PPL1 cells
0
1
2
3
4
5
6
7
8
9
10
11
12
13
c061;MBGAL80
MBGAL80;krasavietz
NP2758
TH
anti-TH and GFP
C
MBGAL80;krasavietz/uas-CD8::GFP
D
MBGAL80/THGAL80;
krasavietz/uas-CD8::GFP

Fig. S5

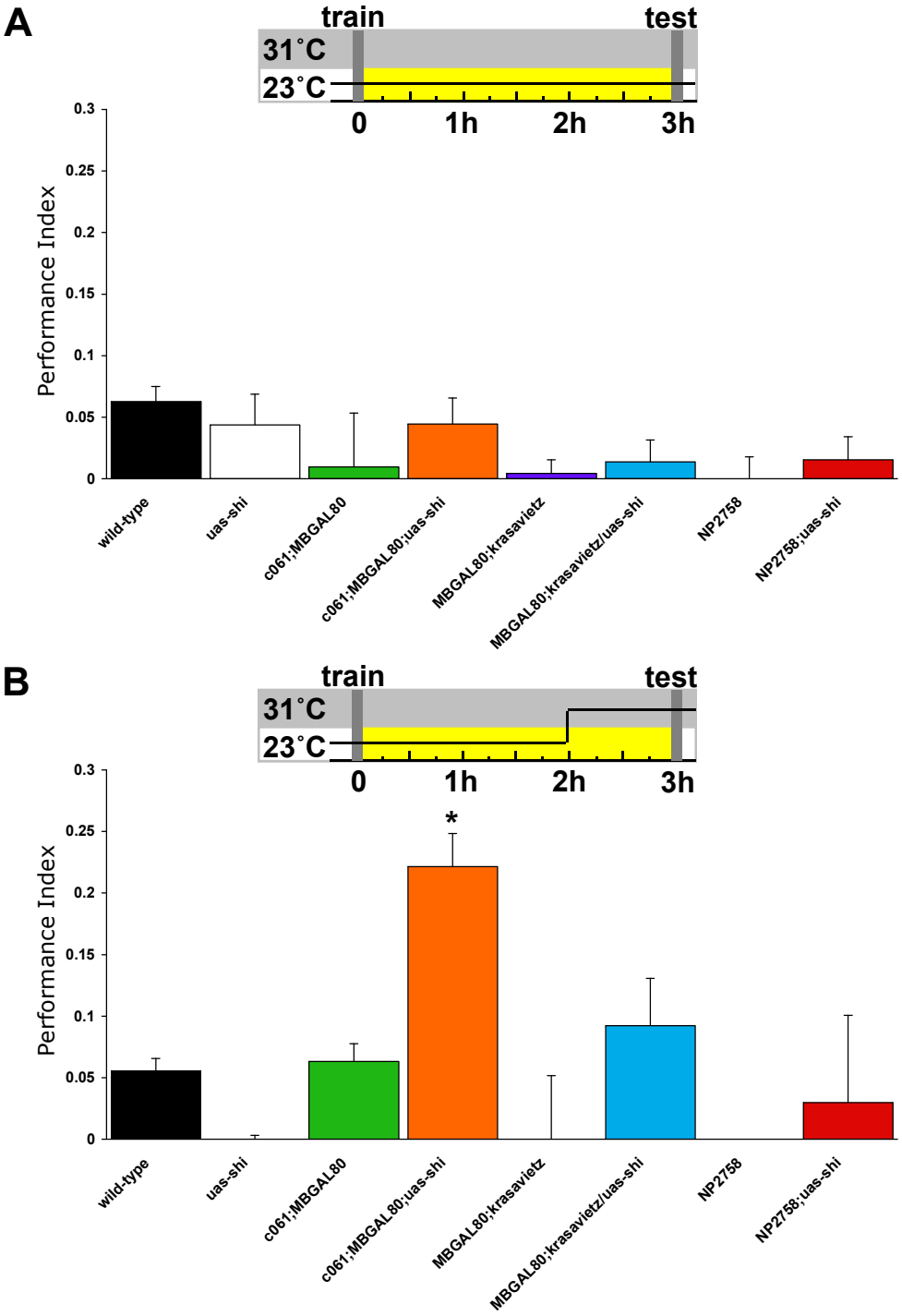
A
train
test
31˚C
23˚C
0
1h
2h
3h
Performance Index
0.3
0.25
0.2
0.15
0.1
0.05
0
wild-type
uas-shi
c061;MBGAL80
c061;MBGAL80;uas-shi
MBGAL80;krasavietz
MBGAL80;krasavietz/uas-shi
NP2758
NP2758;uas-shi
B
train
test
31˚C
23˚C
0
1h
2h
3h
*
Performance Index
0.3
0.25
0.2
0.15
0.1
0.05
0
wild-type
uas-shi
c061;MBGAL80
c061;MBGAL80;uas-shi
MBGAL80;krasavietz
MBGAL80;krasavietz/uas-shi
NP2758
NP2758;uas-shi

Fig. S6

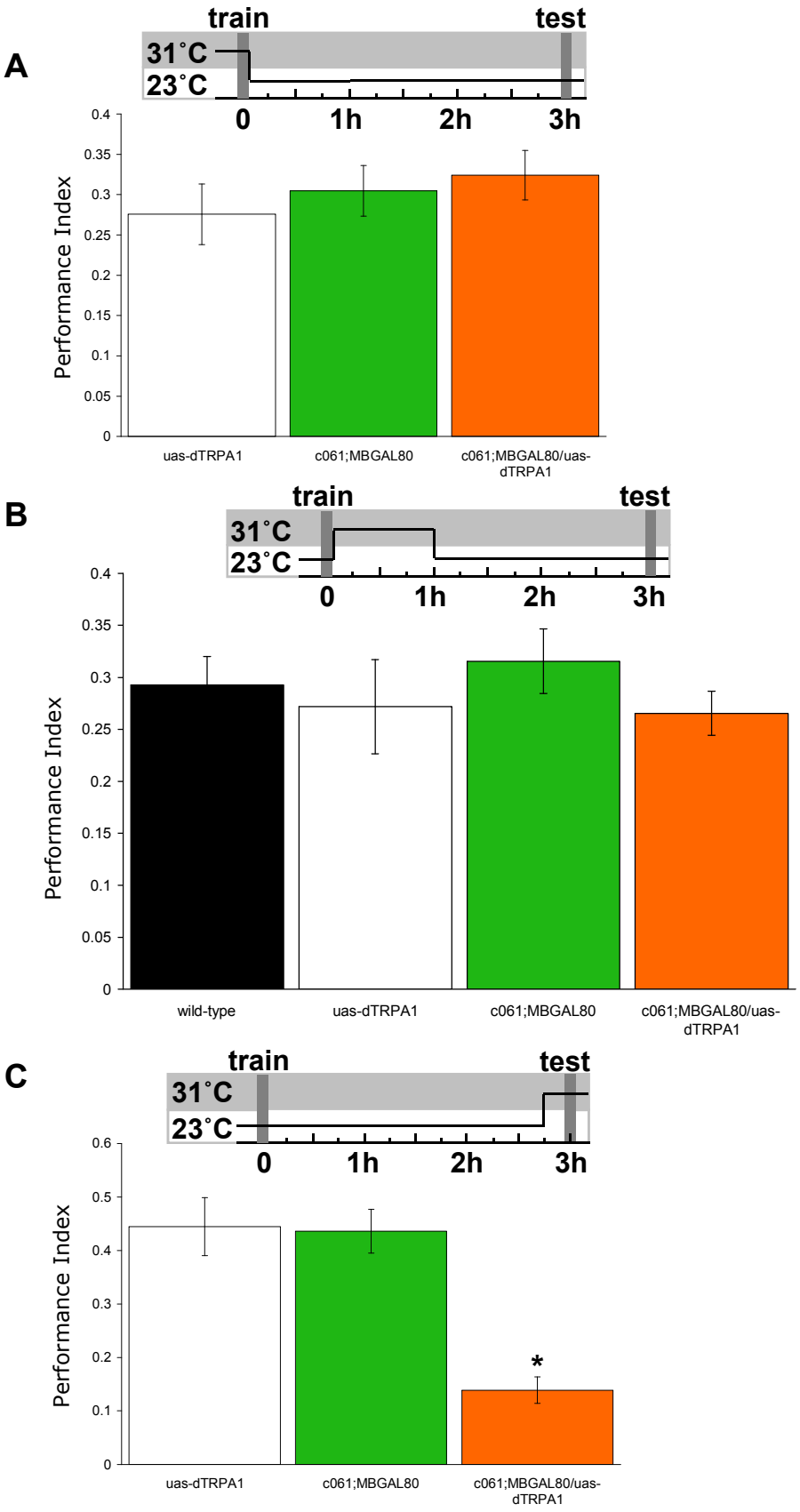
A
train
test
31˚C
23˚C
0
1h
2h
3h
Performance Index
0.4
0.35
0.3
0.25
0.2
0.15
0.1
0.05
0
uas-dTRPA1
c061;MBGAL80
c061;MBGAL80/uas-dTRPA1
B
train
test
31˚C
23˚C
0
1h
2h
3h
Performance Index
0.4
0.35
0.3
0.25
0.2
0.15
0.1
0.05
0
wild-type
uas-dTRPA1
c061;MBGAL80
c061;MBGAL80/uas-dTRPA1
C
train
test
31˚C
23˚C
0
1h
2h
3h
Performance Index
0.6
0.5
0.4
0.3
0.2
0.1
0
*
uas-dTRPA1
c061;MBGAL80
c061;MBGAL80/uas-dTRPA1

Fig. S7

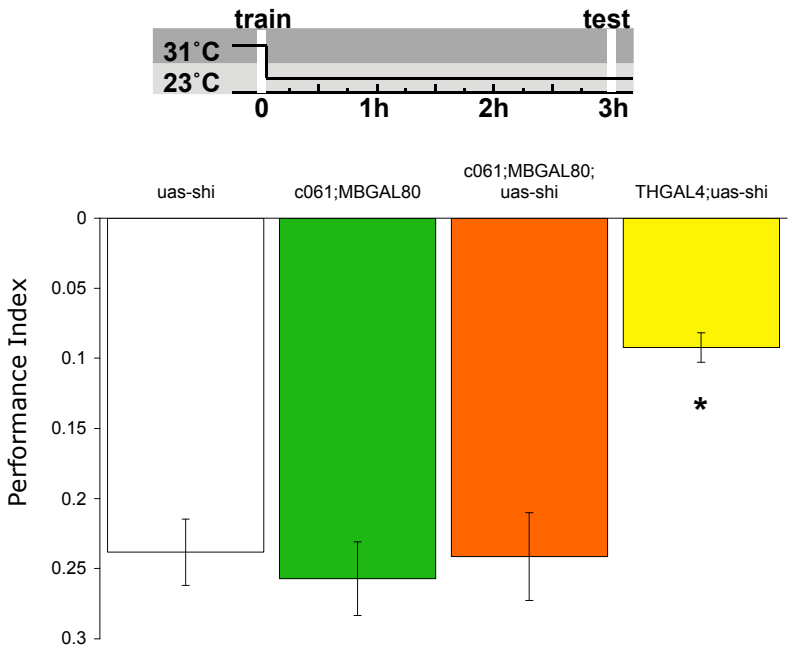
train
test
31˚C
23˚C
0
1h
2h
3h
uas-shi
c061;MBGAL80
c061;MBGAL80;
uas-shi
THGAL4;uas-shi
Performance Index
0
0.05
0.1
0.15
0.2
0.25
0.3
*